Supplemental Information

Cell autonomous versus systemic Akt isoform deletions uncovered new roles for Akt1 and Akt2 in breast cancer

Xinyu Chen, Majd M. Ariss, Gopalakrishnan Ramakrishnan, Veronique Nogueira, Catherine Blaha, William Putzbach, Abul B. M.M. K. Islam, Maxim V. Frolov, and Nissim Hay

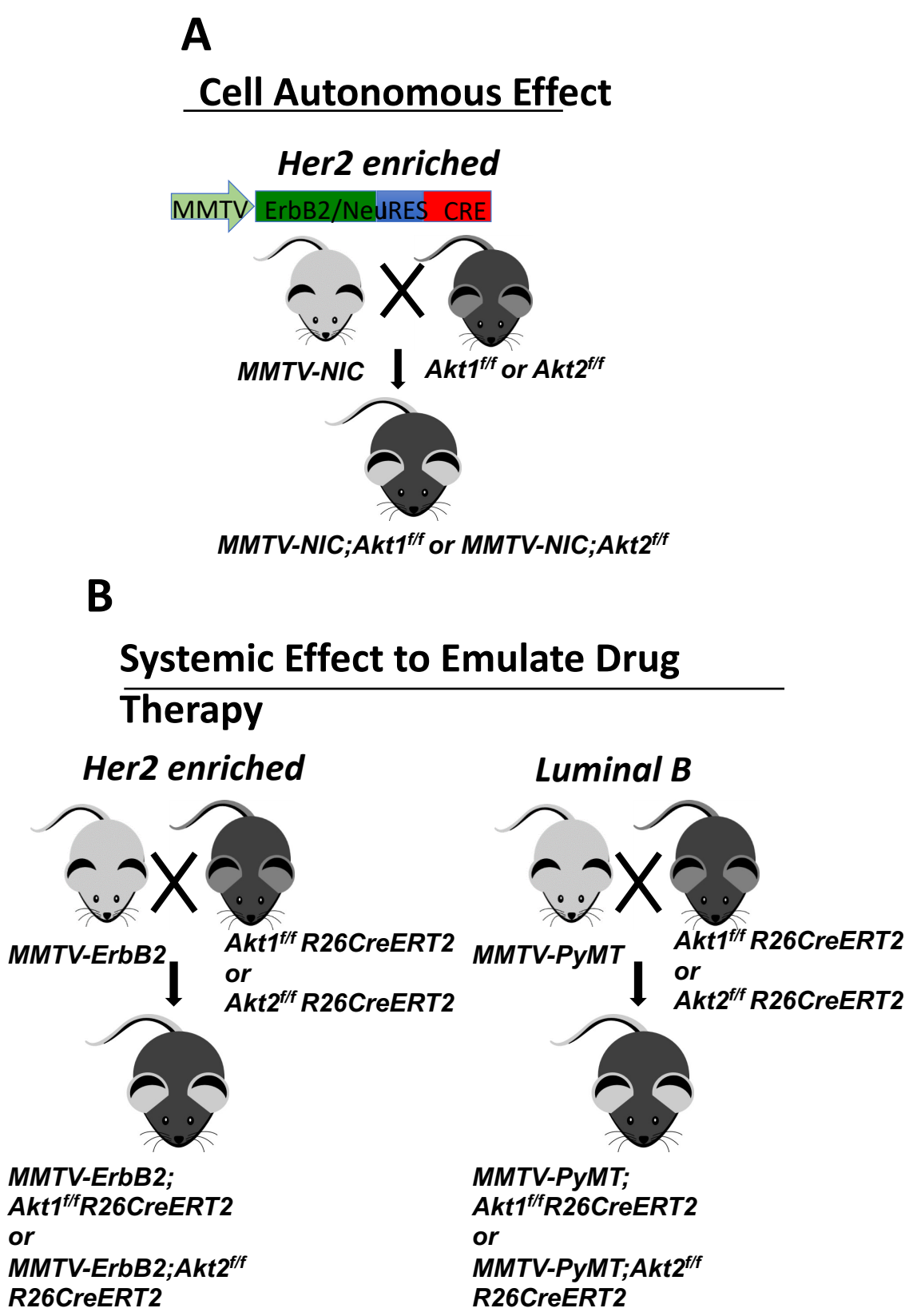

Figure S1 – related to Figures 1, 2, and 3: Breeding schemes. A. Breeding scheme to generate a high Her2 mouse model with mammary gland-specific deletion of Akt1 or Akt2 to determine the cell autonomous effect. **B.** Breeding scheme to determine the systemic effect of Akt1 or Akt2 deletion in high Her2 (left panel) and luminal B (right panel) mouse models.

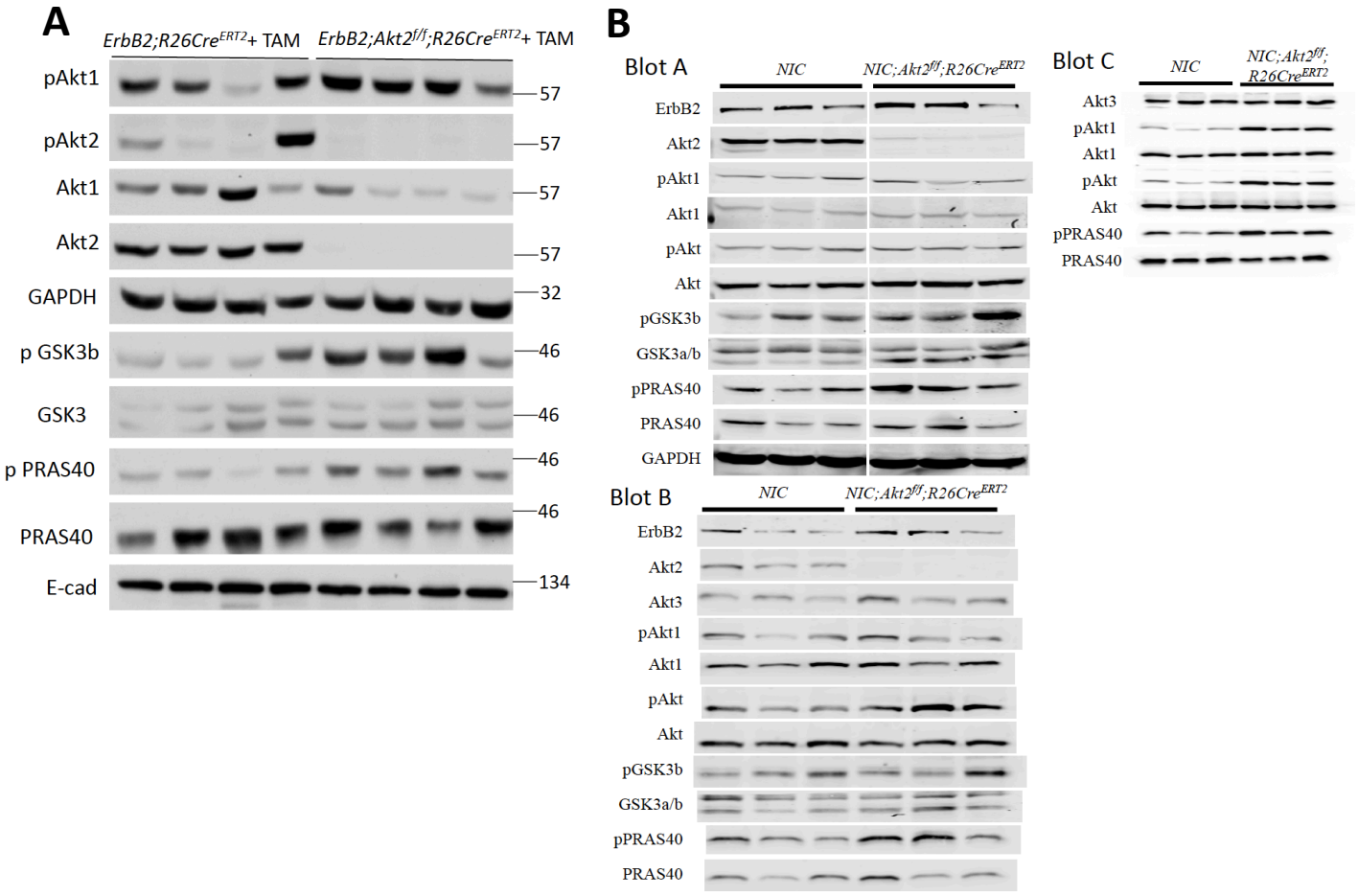

Figure S2 - related to Figure 2: A. Representative immunoblot showing the phosphorylation of Akt1 (pSer473), GSK3b, and PRAS40 in mammary gland tumors derived from control *MMTV-ErbB2;R26Cre^{ERT2}* or *MMTV-ErbB2;Akt2$^{f/f}$;R26Cre^{ERT2}* mice after the systemic deletion of Akt2. Protein extracts from individual tumors in four different mice were used. Immunoblots were used for quantifications in Fig. 2G. **B.** Representative immunoblots showing expression of Akt1, Akt2, Akt3, and total Akt, GSK3b, PRAS40, phosphorylation of Akt1 (pSer473), phosphorylation of pan-Akt (pSer473), phosphorylation of GSK3b, and PRAS40 in mammary gland tumors derived from control *MMTV-NIC or MMTV-NIC;Akt2$^{f/f}$;R26Cre^{ERT2}* mice after the systemic deletion of Akt2. Protein extracts from individual tumors in nine different mice were used. Immunoblots were used for quantifications in Fig. 2I.

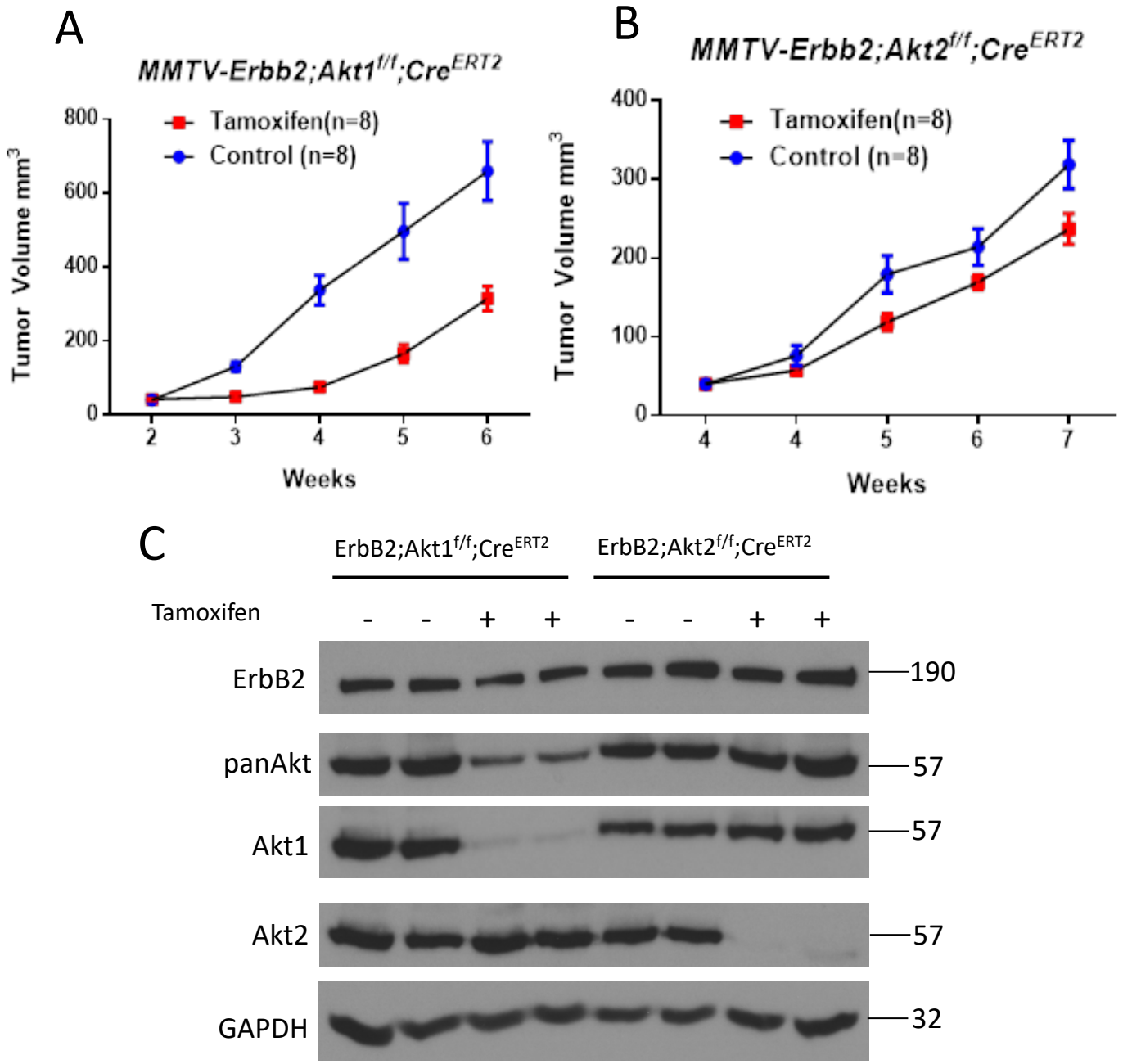

Figure S3 – related to Figure 1 and Figure 2: Cell autonomous deletion of Akt1 or Akt2 in orthotopically transplanted tumors in NOG mice. A. Tumor growth curve of mammary tumor cells derived from *MMTV-ErbB2;Akt1$^{f/f}$;R26RCre^{ERT2}* mice and orthotopically implanted into the mammary fat pad of NOG mice. After palpation, the mice were either treated or not treated with tamoxifen to delete Akt1. Cell autonomous Akt1 deletion significantly impaired tumor growth (n=8, $p<0.001$). **B.** Tumor growth curve of mammary tumor cells derived from *MMTV-ErbB2;Akt2$^{f/f}$;R26RCre^{ERT2}* mice and orthotopically implanted into the mammary fat pad of NOG mice. After palpation, the mice were either treated or not treated with tamoxifen to delete Akt2. Cell autonomous Akt2 deletion significantly impaired tumor growth (n=8, $p<0.001$). **C.** Representative immunoblot showing the level of total Akt expression in orthotopic tumors after the deletion of Akt1 or Akt2.

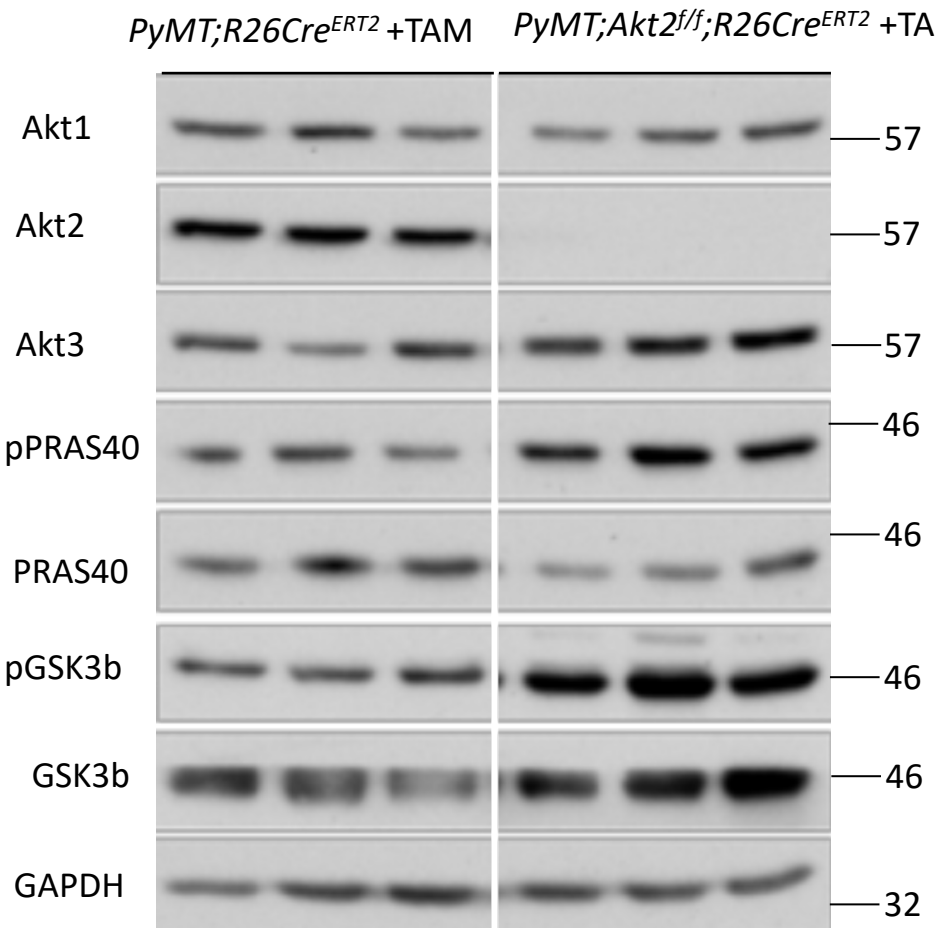

Figure S4 – related to Figure 3F: Representative immunoblot showing the phosphorylation of GSK3b and PRAS40 in mammary gland tumors derived from control *MMTV-PyMT;R26Cre^{ERT2}* mice or after the systemic deletion of Akt2. Extracts from individual tumors in three different mice were used.

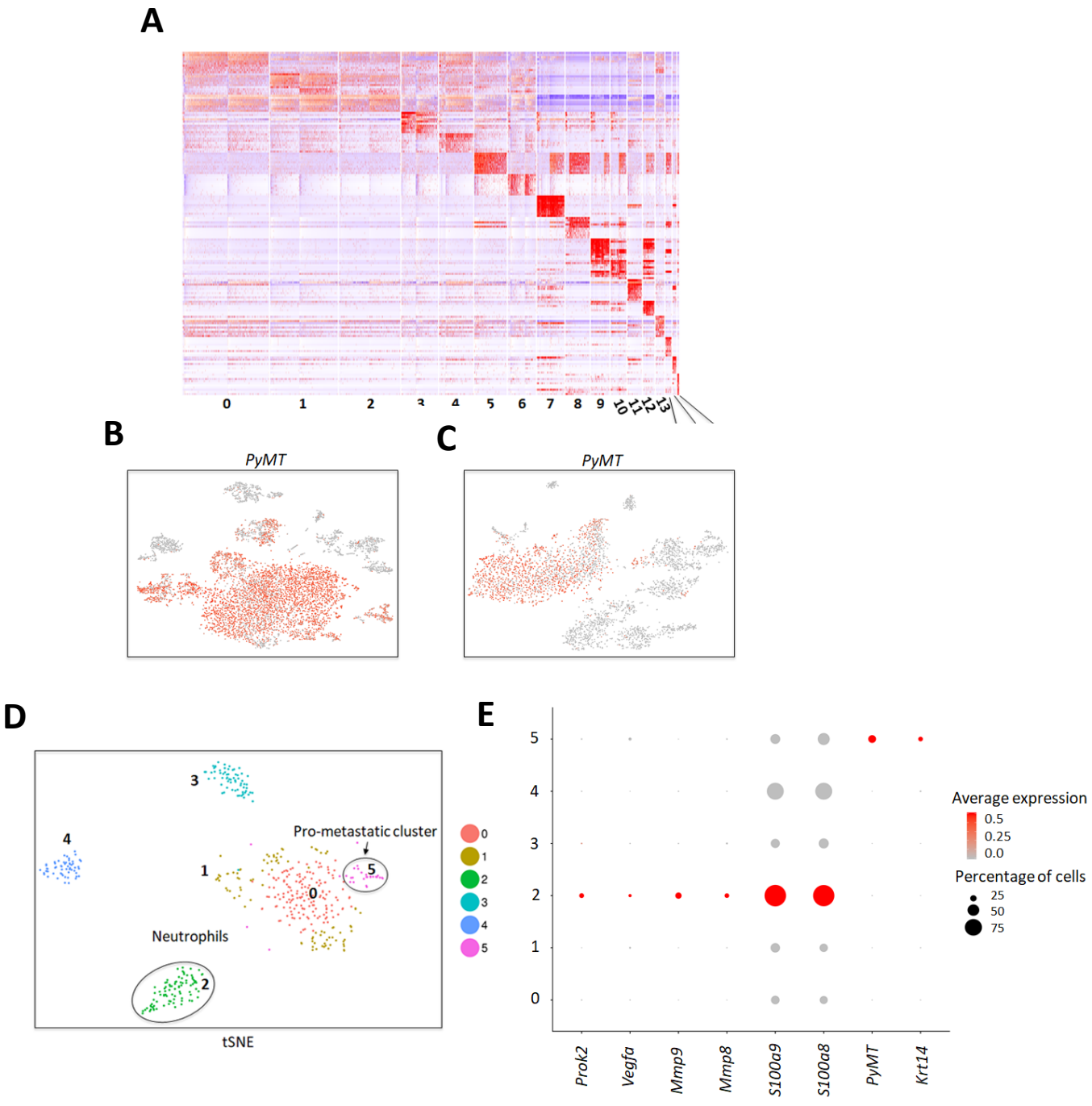

Figure S5 – related to Figure 4: **A.** Heatmap showing distinct markers in each cluster using scRNA-seq on the primary *MMTV-PyMT* breast tumor tissue. **B.** Feature plot showing the cells expressing *PyMT* (in salmon) in the primary breast tumor analysis. **C.** Feature plot showing the cells expressing *PyMT* (in salmon) in the metastatic lung tumor analysis. **D.** Analysis of lung micrometastatic lesions revealing prometastatic cluster 5 and the pro-metastatic neutrophils cluster 2. **E.** Dot plot showing the expression of *PyMT* and *Krt14* in cluster 5 only in the micrometastasis analysis, and *Prok2, Vegfa, Mmp9, Mmp8, S100a9, S100a8* in neutrophil cluster 2.

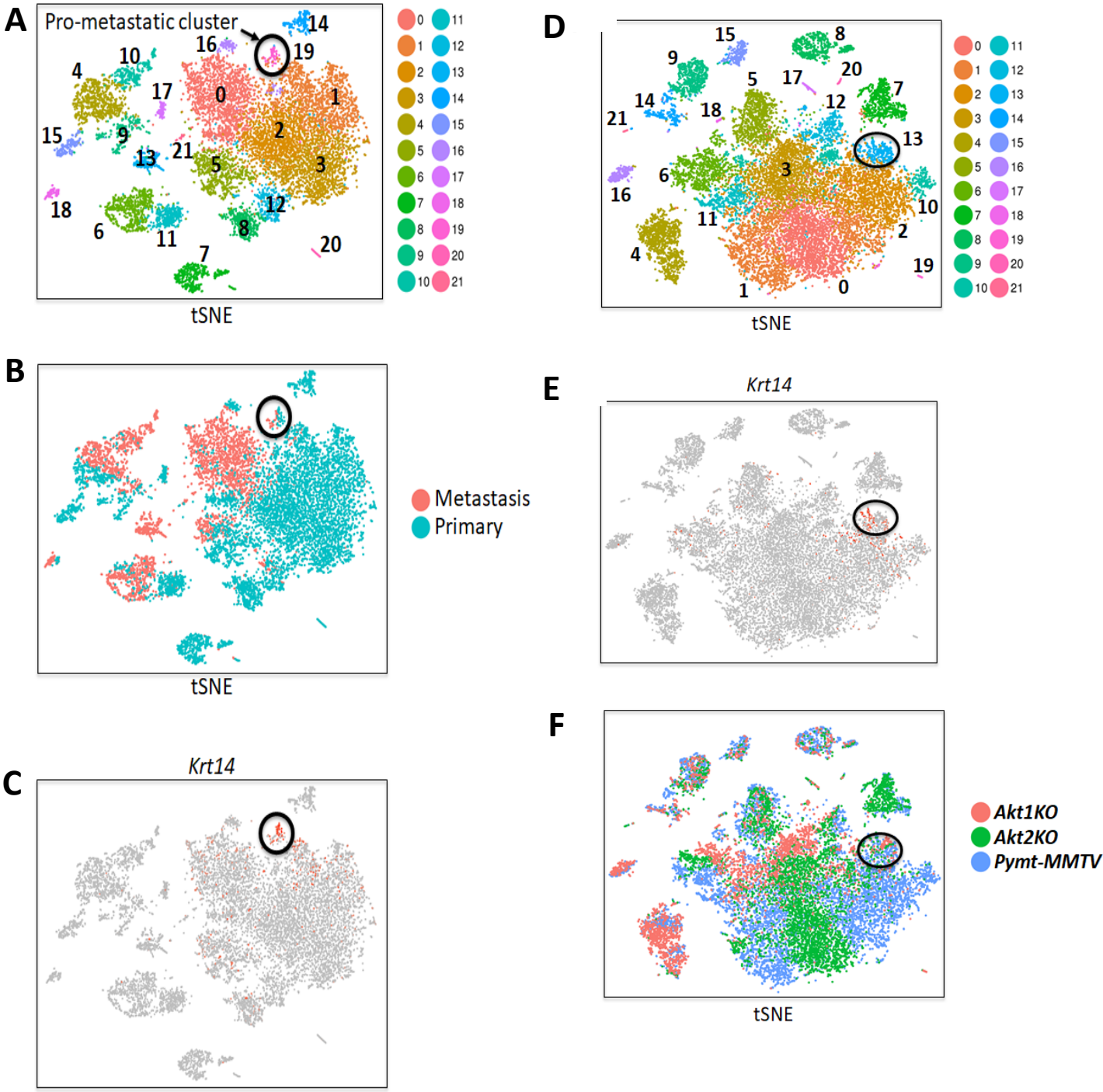

Figure S6 – related to Figure 4: A. A combined tSNE plot of 7,791 primary breast tumor cells (N = 5) and 3,979 metastatic lung tumor cells (N = 3). Cluster 19 - the pro-metastatic cluster is circled. **B.** tSNE showing the cell of origin of the analysis in A. The circle shows that cluster 19 is made of both wild type (WT) primary breast cells in blue and metastatic lung (met) cells in salmon. **C.** Feature plot showing expression of *Krt14* on the tSNE localized in cluster 19. **D.** A combined tSNE plot of 7,791 primary breast tumor cells (N = 5), 3,194 cells of primary tumors following systemic *Akt1* deletion (N = 3), and 4,647 cells of primary tumors following systemic *Akt2* deletion (N = 3). Cluster 13 - the pro-metastatic population, is circled. **E.** Feature plot showing the expression of *Krt14* on the tSNE localized in cluster 13. **F.** tSNE showing the cell of origin of the analysis in A. The circle shows that cluster 13 consists of WT cells in blue, systemic *Akt1* deletion in salmon, and systemic *Akt2* deletion in green.

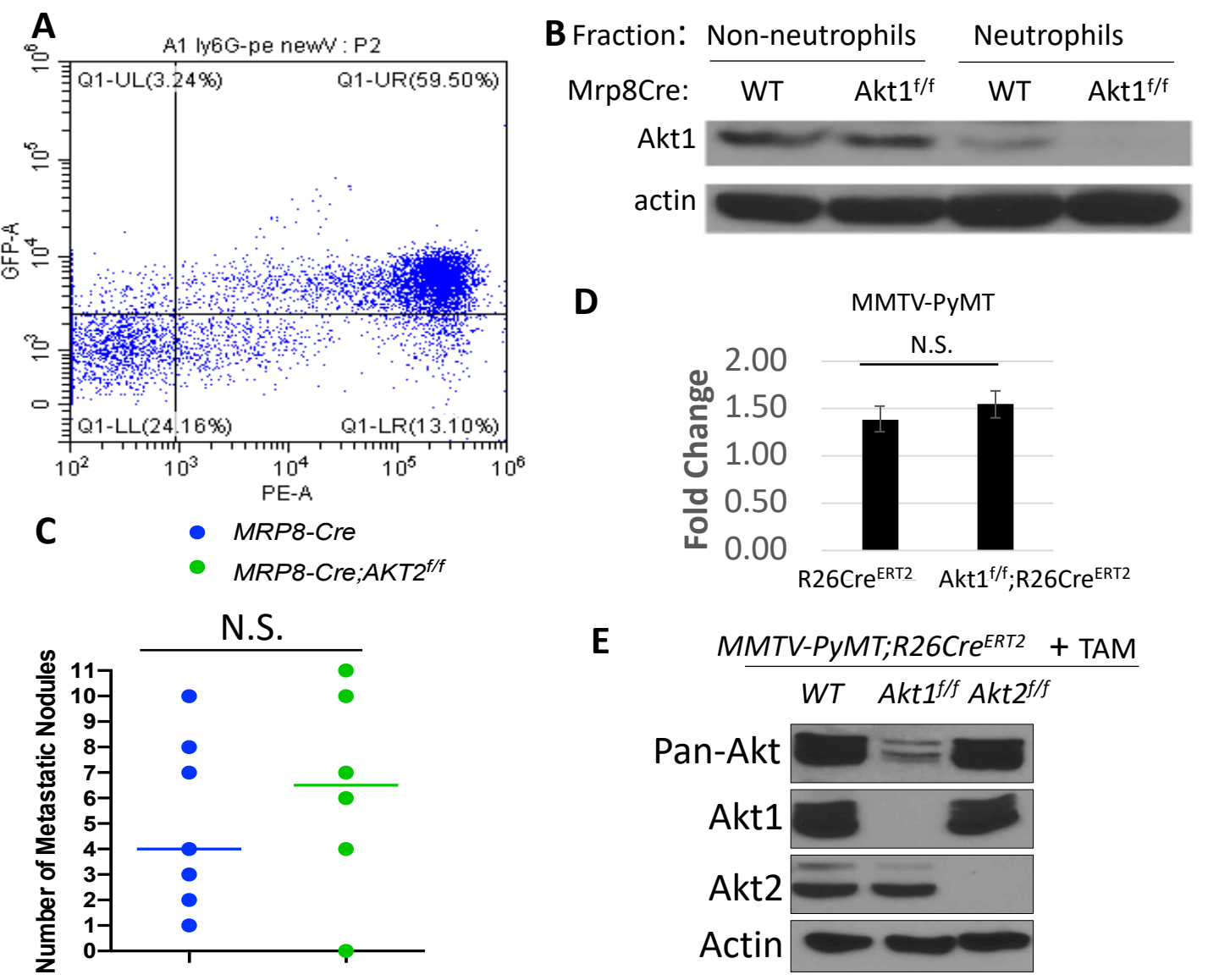

Figure S7 – related to Figure 6: A. Cells with Surface Expression of Ly6G Selectively Express GFP driven by MRP8. Total bone marrow cells were surface stained with PE anti-mouse Ly6G antibody, followed by flow cytometric analysis to correlate cells expressing Ly6G, which is specific for neutrophils, and GFP driven by MRP8 promoter. The LL quadrant represents cells negative for Ly6G and GFP. UL are cells negative for Ly6G and positive for GFP. UR are cells positive for both Ly6G and GFP. LR are cells positive for Ly6G and negative for GFP. Quadrants were set with bone marrow cells that lacked any expression of GFP. **B. Immunoblot showing the specific deletion of Akt1 in neutrophils.** Bone marrows were isolated from control Mrp8Cre (WT) and *Mrp8Cre;Akt1$^{f/f}$* mice. Neutrophils were separated from the rest of the bone marrow cells with Ly6G magnetic beads. Protein extracts from the non –neutrophils fraction and neutrophils fraction were subjected to immunoblotting with anti-Akt1 antibodies. **C.** The effect of Akt2 deletion on metastasis in *MRP8-Cre* mice after orthotopic transplantation of E0771 cells. **D.** The effect of G-CSF on the level of Mcl1 mRNA in neutrophils isolated from control or systemically deleted tumor-bearing mice in Fig. 6C. **E.** Immunoblot showing total Akt expression (pan-Akt) in neutrophils isolated from either control (WT) or systemically deleted Akt1 or Akt2 tumor-bearing mice.